Available online at www.sciencedirect.com

SciVerse ScienceDirect

Journal of the European Ceramic Society 32 (2012) 1575–1583

www.elsevier.com/locate/jeurceramsoc

Tailored graded pore structure in zirconia toughened alumina ceramics using double-side cooling freeze casting

Annemarie Preiss [a], Bo Su [a,*], Simon Collins [b], David Simpson [b]

[a] *Biomaterials Engineering Group (bioMEG), School of Oral & Dental Sciences, University of Bristol, UK*
[b] *Corin Group PLC, The Corinium Centre, Cirencester, UK*

Received 15 September 2011; received in revised form 12 December 2011; accepted 28 December 2011
Available online 20 January 2012

Abstract

Ceramics with graded and continuously aligned open pores were investigated using a double-side cooling freeze casting setup. The ceramic preforms with tailored lamellae spacing (wavelength), wall thickness and graded pore structure were used to infiltrate with a second phase for the fabrication of graded interpenetrating phase composites. The effects of solid content, temperature setting and gradient, cooling rate and the introduction of electrophoretic deposition (EPD) on the freezing velocity of the ceramic suspension were analysed. On the bottom of the ceramic specimen, a dense layer was formed and tailored with the use of EPD. The ceramic was characterised by a graded open pore structure with wavelengths up to 115 μm and interconnected microstructure. The effect of solid content on the degree of supercooling and the effect of temperature gradient on the average freezing velocity were investigated. The addition of EPD before freeze casting affected significantly the microstructure, the wavelength decreased and the wavelength gradient became smaller compared to simple freeze casting.

Keywords: Freeze casting; Microstructure; Porosity; Al_2O_3; Suspensions

1. Introduction

Ceramics with a tailored graded pore structure can be used for filtration devices and planar solid oxide fuel cells (SOFC).[1–6] They can also be employed as preforms to infiltrate with a second phase such as polymer or metal to fabricate functionally graded composites used for orthopaedic implants and other engineering applications. Typical methods to produce open porous ceramics are replication, direct foaming or templating. The replication method involves the coating of a structured substrate (e.g. a polyurethane sponge) with a ceramic suspension followed by substrate removal using thermal treatment; however the main drawback is that through the pyrolysis of the substrate the struts become void which decreases the mechanical strength of the ceramic body.[7–9] In direct foaming, air is either blown into a ceramic suspension or bubbles are directly produced in the slurry via chemical processes that produce gas. The technique has however disadvantages such as low permeability due to small windows on the pore walls, low homogeneity and difficulty of achieving graded structure in the ceramic body.[3,8–10] Freeze casting is an alternative route that offers versatility, low cost and is environmentally friendly.[11] In freeze casting based on aqueous suspension, ice crystals grow in the ceramic suspension and particles accumulate between the ice columns. The crystals are served as templates for the pores and are removed through freeze drying. Importantly, it is possible to produce graded pore structures.

Over the last decade the freeze casting process has attracted considerable attention in a wide range of fields with different kinds of materials such as ceramics, polymers and metals being used.[4,12–18] The popularity of this process has grown due to easily tuneable microstructures by varying process parameters resulting in very complex and sophisticated structures.

Unidirectional freeze casting of ceramics in a single cooled system has been widely investigated by many research groups.[19–23] But since the freeze casting process is a highly sensitive method the microstructure of ceramics is easily influenced by small temperature changes, it is essential to build a system which is appropriately insulated by the surrounding temperature fluctuation. A closed system, in which both, bottom and top, rod

* Corresponding author. Tel.: +44 0117 3424361; fax: +44 0117 3424313.
E-mail addresses: a.preiss@bristol.ac.uk (A. Preiss), b.su@bristol.ac.uk (B. Su), simon.collins@coringroup.com (S. Collins), david.simpson@coringroup.com (D. Simpson).

0955-2219/$ – see front matter © 2012 Elsevier Ltd. All rights reserved.
doi:10.1016/j.jeurceramsoc.2011.12.031

temperatures are controlled, is a relatively new attempt which was used by Deville et al.[4,24] and is crucial for the reproducibility of the ceramic specimen.[25]

In freeze casting, the initial freezing is very fast. Ice engulfs the ceramic particles instead of forming columnar and lamellar structures. The growing ice front is planar with trapped ceramic particles, which results in the formation of a relatively dense layer on the bottom of the sample.[4] To increase the density and thickness of this layer, an electric field can be used during freeze casting as Zhang et al.[26] reported. They used a combination of EPD and unidirectional freeze casting to fabricate dense/porous ceramic bi-layers. The dense layer was tuned by the electric potential and the ceramic lamellae spacing was constant over the whole height of the sample.

Most papers and reviews concentrate on the fabrication of aligned lamellae structures with homogeneous distributed porosity.[1,11,27] In terms of ceramics with graded pore structures produced via freeze casting, only few studies were reported.[1,6] Bettge et al.[2] fabricated yttria-stabilised zirconia ceramics with a graded pore structure from 0 to 90%. Sedimentation prior to freeze casting was used to control the pore gradient and dense deposit. However the wavelength and wall thicknesses were restricted as they were about 30 μm and 2–5 μm, respectively. Koh et al.[6] reported the fabrication of dense/porous bi-layered ceramics using a camphene based suspension. Ceramic specimens with dendritic pore channels and a dense layer on one side and pore sizes of about 17 μm on the other were achieved. Sofie,[28] used a combination of freeze casting and tape casting, but the sample thickness was limited.

In this work the focus is on the investigation of tailored graded pore structure in ZTA ceramics using a double-side cooling freeze casting system. To improve the density of the dense layer as well as the thickness, attempt was made on the introduction of an electric field. The graded pore structure was manipulated using a range of processing conditions such as freezing temperatures, cooling rates and solid loadings. The novel freeze casting apparatus, the freezing conditions and the introduction of electrophoretic deposition are discussed.

2. Material and methods

2.1. Raw materials

Alumina powder (CT3000SG, Almatis, USA) with an average particle size of 0.5 μm and zirconia powder (TZ-3YS-E, yttria partially stabilised, Tosoh Corp., Japan) with an average particle size of 0.3 μm were used in this study. Aqueous suspensions containing 15–35 vol% zirconia toughened alumina (ZTA) with 10 wt% zirconia relative to alumina were dispersed in distilled water using an anionic dispersant, Dolapix CE64 (Zschimmer & Schwarz, Germany), at a ratio of 0.6 wt% of the dry powder weight. To increase the strength of the green ceramic, polyvinyl alcohol (PVA, MW: 30,000–70,000, Sigma–Aldrich, USA) was added at a ratio of 1.5 wt% with respect to the ceramic powder, acting as an organic binder. The mixtures were ball milled in polyethylene bottles using zirconia balls for 12 h to obtain well dispersed suspensions and ultrasonicated for 10 min to break down agglomerates and achieve a consistent homogeneity in the slurry.

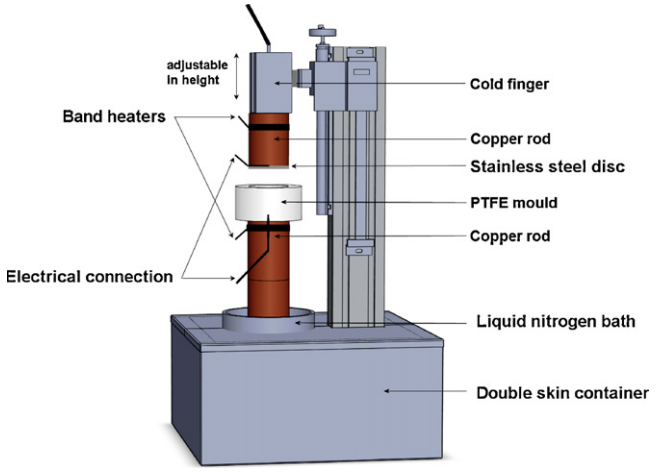

Fig. 1. Schematic illustration of double-side cooling apparatus utilised for unidirectional freeze casting and EPD.

2.2. Apparatus

The apparatus built for the novel process combination of unidirectional freeze casting and EPD consisted of a double-side cooling system, as shown in Fig. 1. The mould was made of a 15 mm thick PTFE ring which insulated the suspension from the sides, and two copper rods (Ø60 mm) used as temperature carriers. A stainless steel (SST) disc was mounted onto the surface of each copper rod which was connected to the pulse generator. The SST discs were electrically insulated from the copper rods to ensure the current flowed only through the ceramic suspension. The bottom thermocouple was in direct contact with the removable SST disc attachment through a slot in the SST disc. The top thermocouple was placed in the copper rod close to the SST disc which was glued onto the copper rod using a thin epoxy resin. Since the discs were in direct contact with the suspension, SST was chosen as it has a higher corrosion resistance compared to copper. The apparatus contained a clear glass window, built into the side of the PTFE mould, enabling the ice front to be monitored during freezing. The window allowed the degree of supercooling (start of solidification) and freezing velocity to be measured by recording the time of solidification. The top rod was cooled using an immersion cooler (FT200, Julabo, Germany), the bottom rod was immersed in a liquid nitrogen bath. The temperatures were controlled through band heaters (MI, 400W, Watlow, USA) and thermocouples (type J, Watlow, USA) placed close to the suspension surfaces. Both rods had the same temperature when the suspension was poured into the mould. The bottom rod was cooled down at a controlled rate of 1 or 2 °C/min whilst the temperature of the top rod was kept constant. Solidification took place unidirectionally, starting from the bottom to the top rod.

The processes of anodic EPD and freeze casting were easily combined once the apparatus was built. To apply an electric field, the temperature controlled upper and lower surfaces were

connected to a waveform generator (33220A, Agilent Technologies, USA) with which a pulsed DC potential was applied to minimise electrolysis of the aqueous suspension. EPD was carried out at a potential of 10 V. A square wave pulse was used with a pulse frequency of 20% duty cycle (dc) and pulse width of 0.005 s. EPD was applied prior to the start of freeze casting. The deposition time was 10 min whereas the actual deposition time was much shorter since a series of direct current pulses of equal amplitude and duration by periods of zero current were applied. To ensure conformity the electrode distance was kept constant with 12 mm throughout the experiments.

2.3. Processing and characterisation

The zeta potential of ceramic suspension was measured using a Zetasizer (Nanoseries Nano-Z, Malvern, UK). Rheological properties of suspensions with different solid contents were measured at 25 °C using a Rheometer (Gemini 200, Bohlin Instruments, UK) at controlled shear rate in a range of 0.1–500 s^{-1} with a cone-plate geometry.

During freeze casting, ceramic particles were rejected by the ice crystals and accumulated between the ice columns. The average freezing velocity was calculated by measuring the time required for solidification. After solidification, the consolidated green ceramic was freeze-dried (Edwards, Modulyo freeze dryer, UK) for 12 h to allow the ice to sublimate. The green ceramics were sintered (Elite thermal systems Ltd., UK) using the following regime: the temperature was first increased, at a heating rate of 1 °C/min, to 600 °C and held for 2 h, followed by a further increase in temperature, at a heating rate of 10 °C/min, to 1600 °C and held for a further 2 h.

The microstructure of the sintered bodies was observed by digital microscopy (KH-7700, Hirox, USA) and scanning electron microscopy (SEM) (JEOL, JSM 6330F, Tokyo, Japan). Ceramic samples were infiltrated with a coloured epoxy resin to give a better contrast. The resin infiltrated samples were cut parallel and perpendicular to the freezing direction, grinded and polished.

3. Results

The zeta potential measurements of the ceramic suspension indicated that the particles are negatively charged at its inherent pH of 9.4 and has its isoelectrical point (IEP) at 5.7 (Fig. 2). Therefore the suspension could be used at its inherent pH for anodic EPD as it is stable with a zeta potential of −43 mV.

The freeze casting experiments showed that 35 vol% was the maximum solid content in suspension that was still easily castable. At a higher solid content, freeze casting of the ceramic specimen produced samples exhibiting poor quality lamellae structure and delamination in the freezing direction, which is attributed to the high viscosity of the suspension. The force with which the ice crystals grow is insufficient to push upwards through the suspension as discovered by Peppin et al.[29] The results of the rheological properties of slurries with different solid content are shown in Fig. 3. The graph indicates that the viscosity of the 45 vol% suspension was 7 times higher at high

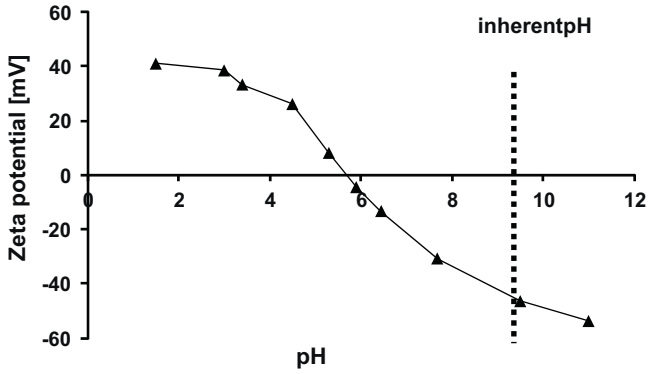

Fig. 2. Zeta potential of ceramic suspension as a function of pH.

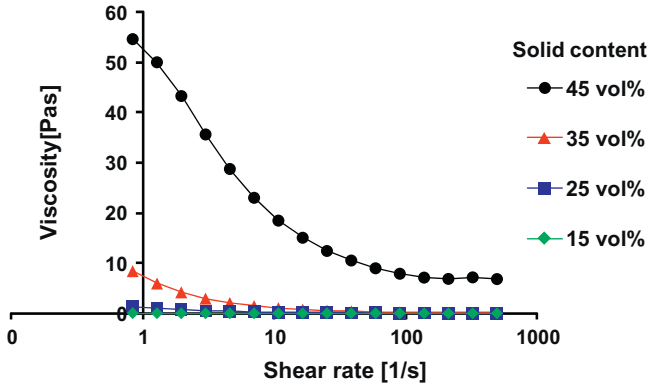

Fig. 3. Rheological curves of ceramic suspensions showing the effect of various solid contents on viscosity.

shear rates between 100 and 500 s^{-1} and increases with decreasing shear rate up to 55 times compared to suspensions with lower solid content which made it impossible to achieve an aligned lamellae porous structure.

Further rheological tests on slurries showed that the viscosity was not greatly affected by temperature between 25 and 5 °C, which was important for the freeze casting process, to ensure the regular growth of the ice crystals during freezing in a given suspension.

Ceramic samples with graded pore structures were investigated and the influence of solid content, freezing velocity and degree of supercooling on the final pore microstructure has been taken into consideration. Fig. 4a shows the degree of supercooling as a function of solid content. The degree of supercooling is the difference between the "real" freezing point of the liquid (T_m) and the temperature at which solidification occurs. The mould of the freeze casting apparatus contained a clear glass window, enabling the ice front to be optically visible and monitored during unidirectional freezing. This allowed the degree of supercooling and average freezing velocity to be calculated according to the time that the ice front took to travel from the bottom to the top of the suspension. It was observed that, with an increasing solid content in suspension, solidification starts earlier compared to suspensions with lower solid content. At solid contents of 15, 25 and 35 vol% freezing starts at −9, −6.4 and −5 °C, respectively. Furthermore, a change in the solid content

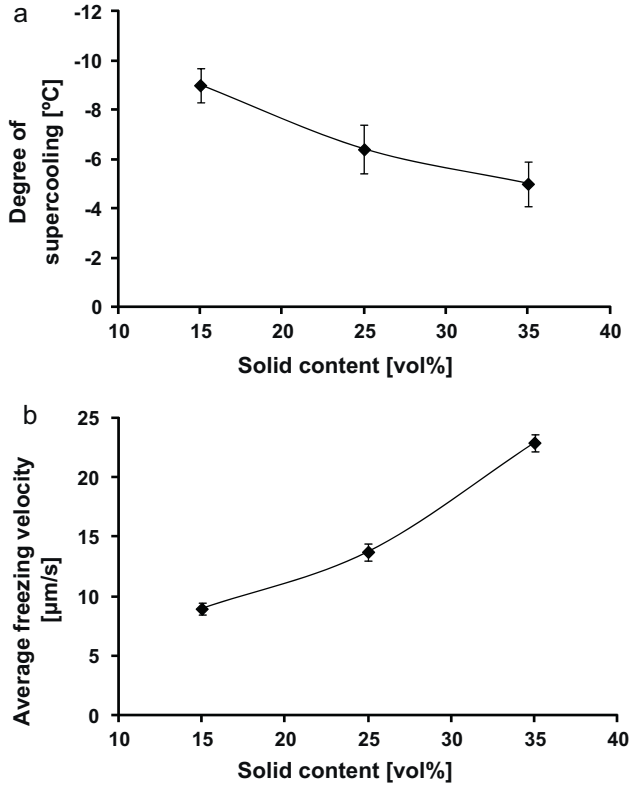

Fig. 4. Effect of solid content on (a) onset freezing temperature and (b) freezing velocity of suspension. Freezing conditions: top temperature: +20 °C, bottom temperature: −10 °C, cooling rate: 1 °C/min.

of the suspension influences the freezing velocity of the ice front and subsequently the microstructure of the specimen as shown in Figs. 4b and 5. With increasing volume fraction the average velocity of the freezing front increases (see Fig. 4b).

Fig. 5 shows cross-sections of ceramic specimens, with a bottom rod temperature of −10 °C and a top rod temperature of +20 °C, at a distance of 8 mm from the bottom rod. The ceramic samples were infiltrated with a coloured resin for better contrast and cut, perpendicular to the freezing direction, every 2 mm to analyse the wavelength and wall thickness at different heights through the sample. The images demonstrate the influence of the suspension content on wavelength and wall thickness. With increasing solid content the wavelength decreases and the wall thickness increases. In Fig. 6 the surface of a typical ceramic wall is shown. It can be seen that the surfaces have a rough structure and in the case of the 35 vol% specimen (Fig. 5c), the distance between the ceramic walls becomes so small that the roughness of the walls was sufficient to bridge adjacent walls.

As seen in Fig. 7, measurement of the wavelength at specific intervals through the ceramic specimens shows that as the distance from the bottom rod was increased, the wavelength of the lamellae also increases. All samples show independently from their solid content a general increase in wavelength with increasing distance to the bottom rod. This is associated to the slowing down of freezing velocity with growing ice front. That means further away from the cold surface the ice growth rate became much lower due to the evolved ice which operates as an insulator and reduces the temperature gradient. The slower the freezing velocity the bigger the wavelengths as the ice

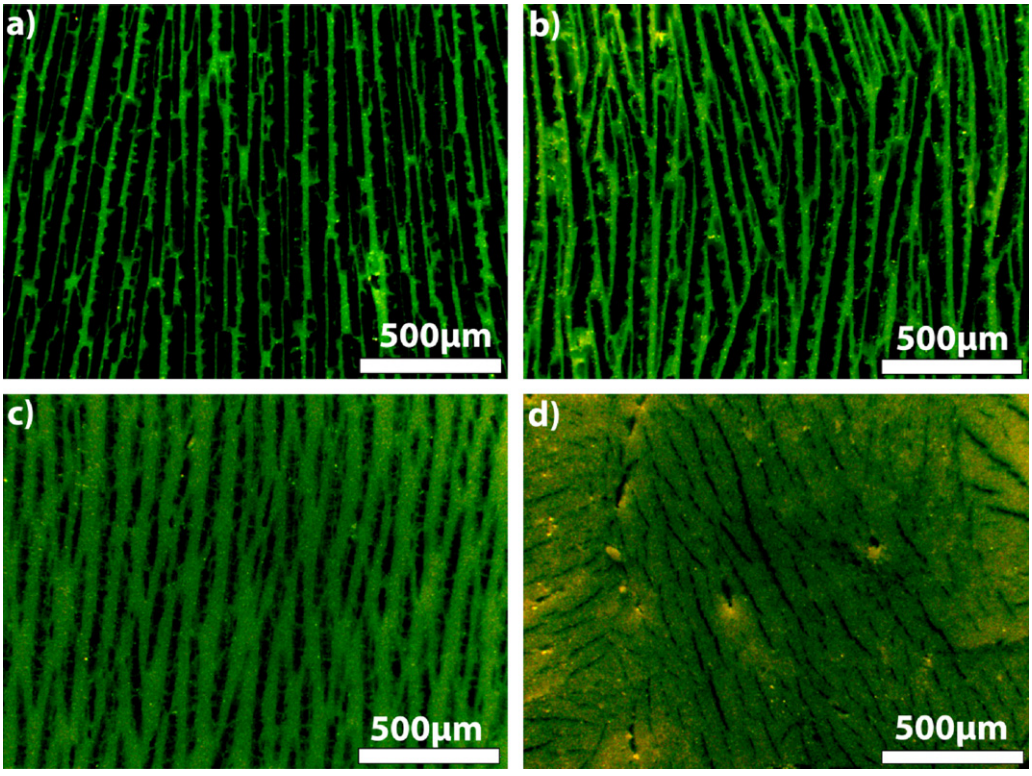

Fig. 5. Cross section of ceramic specimens cut perpendicular to freezing direction at 8 mm height with different solid content, (a) 15 vol%, (b) 25 vol%, (c) 35 vol% and (d) 45%. Freezing conditions: top temperature: +20 °C, bottom temperature: −10 °C, cooling rate: 1 °C/min.

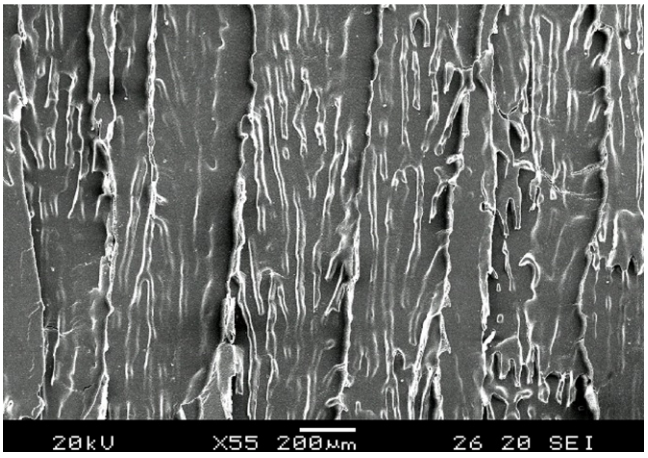

Fig. 6. SEM micrograph of sintered ceramic lamellae surfaces with dendrite structures.

crystals have more time to grow horizontally. Fig. 7a also illustrates that with decreasing solid content the gradient of the wavelength within a sample becomes more significant with one exception for the 35 vol% suspension at 2 mm height. The reason for the very small wavelengths at the bottom of this sample is firstly connected to the high amount of nucleation sites due to the high concentration of ceramic particles in suspension. Secondly, the microstructure is also influenced by the degree of

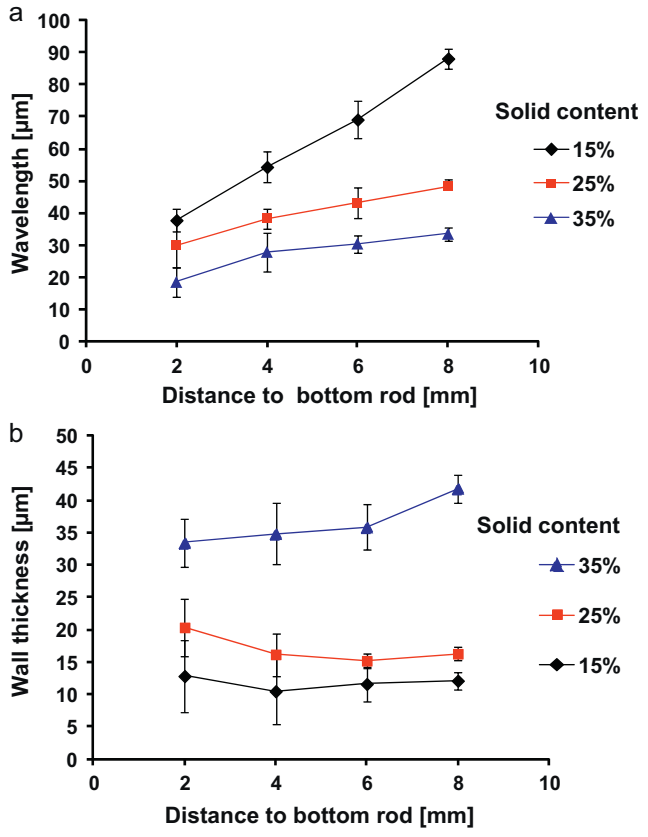

Fig. 7. Influence of solid content on (a) wavelength and (b) wall thickness at different distances to bottom rod. Freezing conditions: top temperature: 0 °C, bottom temperature: −10 °C, cooling rate: 1 °C/min.

supercooling. Freezing generally starts when the nuclei have reached their critical size. Until freezing occurs, the system is in a supercooled state where the temperature of the system is lower than the freezing temperature of the liquid phase; the system is out of equilibrium. A system always tries to reach equilibrium which can be achieved by ice crystal growth. Therefore, the higher the degree of supercooling is, the faster the initial freezing velocity will be in order to obtain the equilibrium temperature. Consequently a narrower wavelength results in the ceramic specimen. Samples with 15, 25 and 35 vol% solid content show an average wavelength of 88, 48 and 33 μm at 8 mm height, respectively.

The decrease in thickness of the ceramic walls, with decreasing solid content (Fig. 7b), is due to the lower number of ceramic particles in suspension. At 35 vol% solid content the average wall thickness was 36.5 μm, at 25 vol% it was 17 μm and at 15 vol% it was 11.8 μm. The 35 vol% samples show an increase in wall thickness with increasing distance to the bottom rod compared to 15 and 25 vol% samples. At a solid content of 35 vol%, a larger number of ceramic particles are present in the suspension; these are not just pushed to the sides during freezing but are also pushed upwards due to lack of space. The wavelength of the ceramic specimens is 14.7, 27.8 and 41.7 μm at 35, 25 and 15 vol%, respectively.

The effect of EPD on the microstructure of the ceramic specimen is shown in Fig. 8. The electric field forced ceramic particles towards the bottom rod where they built a dense layer and at the same time a gradient particle distribution arisen in suspension. Much higher densities on the bottom of the samples can be achieved due to the additional force of the electric field. The number of lamellae was larger in samples, where an electrical field was applied due to an increased number of particles being forced towards the bottom rod. This leads to more nucleation sites which resulted in a larger number of ice crystals being formed and the much finer final structure. A similar effect was observed in slurries of higher solid contents. Not only does the addition of EPD prior to freeze casting results in a smaller wavelength but also at the same time, it causes a decrease in wavelength gradient throughout the sample as shown in Fig. 9. The sample without EPD shows an increase of wavelength from 30 to 47 μm, but an increase with EPD from 25 to 31 μm, at the height from 2 to 8 mm.

The freezing velocity and therefore the microstructure of the resultant ceramic specimen, are dependent on the temperature of the bottom rod and the cooling rate as illustrated in Fig. 10a. It can be seen that the ice front velocity decreased with the decrease of cooling rate, independent of the temperature of the bottom rod. The average freezing velocity of the ice front decreased approximately by 0.1 μm/min when a slower cooling rate was applied, resulting in smaller wavelengths in ceramics.

The influence of the temperature settings on ice front velocity is shown in Fig. 10b. With decreasing top and bottom temperature the ice front velocity increased markedly. When the top temperature was +10 °C instead of +20 °C, the temperature gradient was smaller which led to a lower ice front velocity even though the temperatures were closer to the freezing point of water. When the bottom temperature was −5 °C, the influence

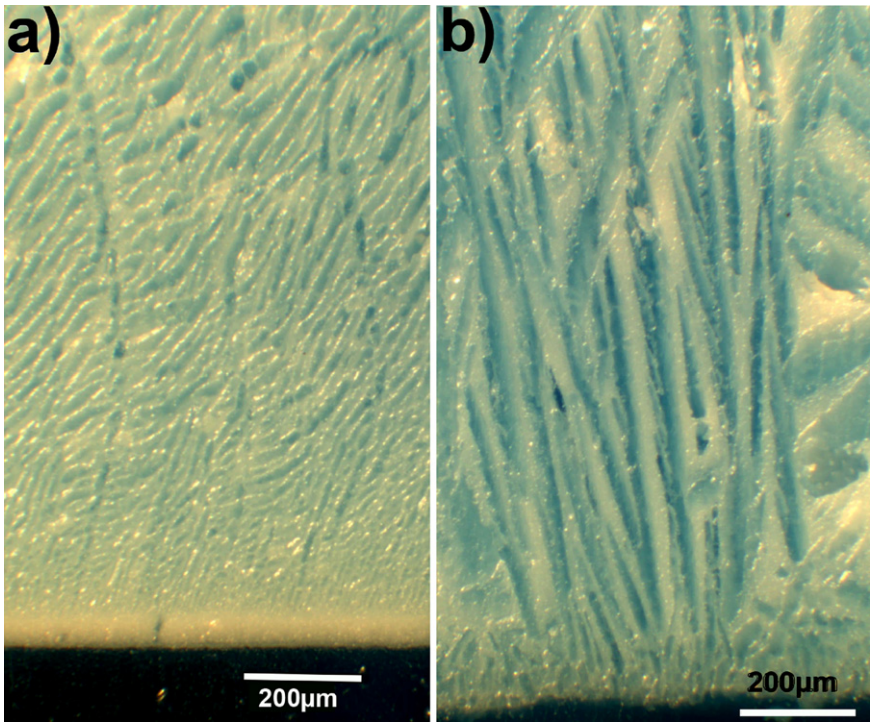

Fig. 8. Microstructure of sintered ceramic cross section parallel to ice growing direction, (a) with EPD, (b) without EPD applied prior to freeze casting.

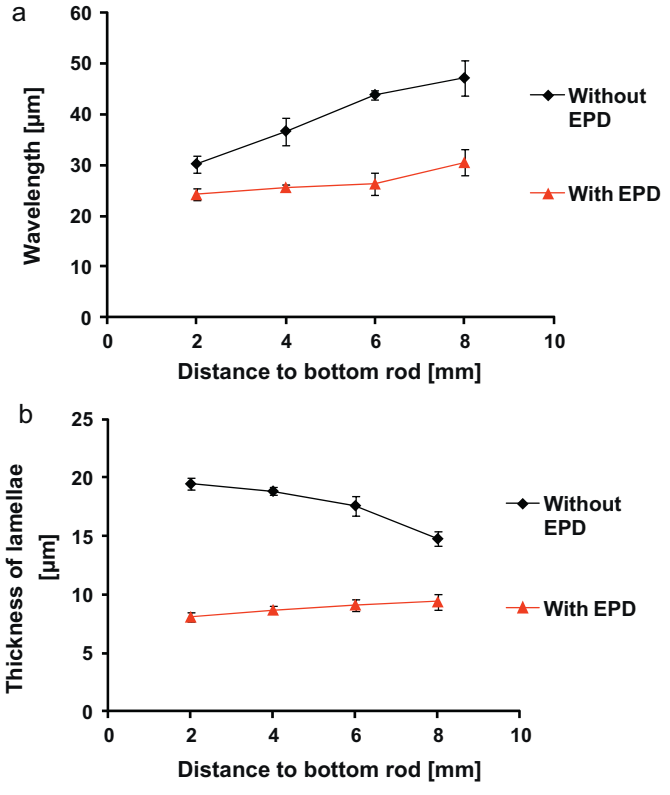

Fig. 9. Influence of EPD on microstructure of freeze cast ceramics at different height. Ceramic solid content: 15 vol%, freezing conditions: top temperature: 0 °C, bottom temperature: −15 °C, cooling rate: 1 °C/min.

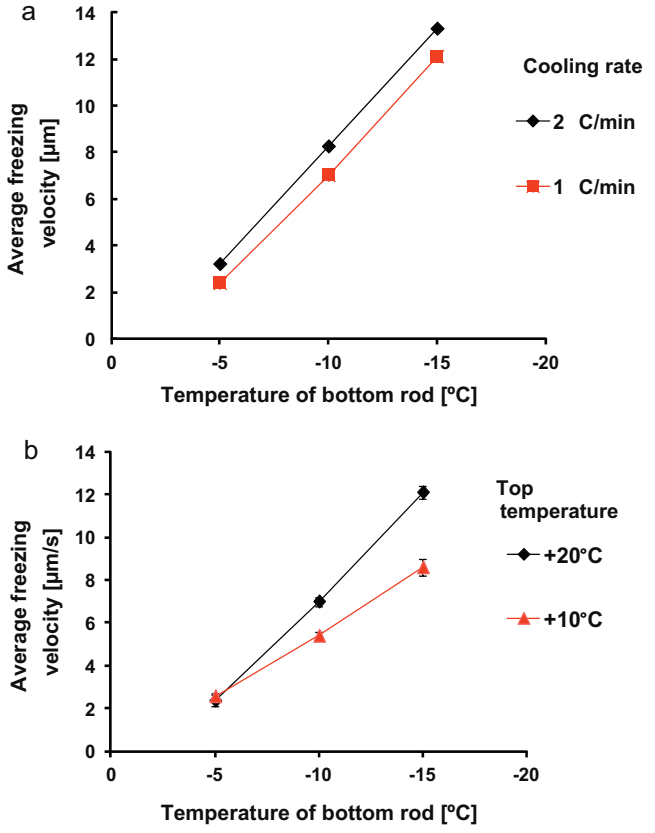

Fig. 10. Influence of (a) cooling rate on freezing velocity (top temperature: 20 °C) and (b) temperature settings on freezing velocity, cooling rate: 1 °C/min.

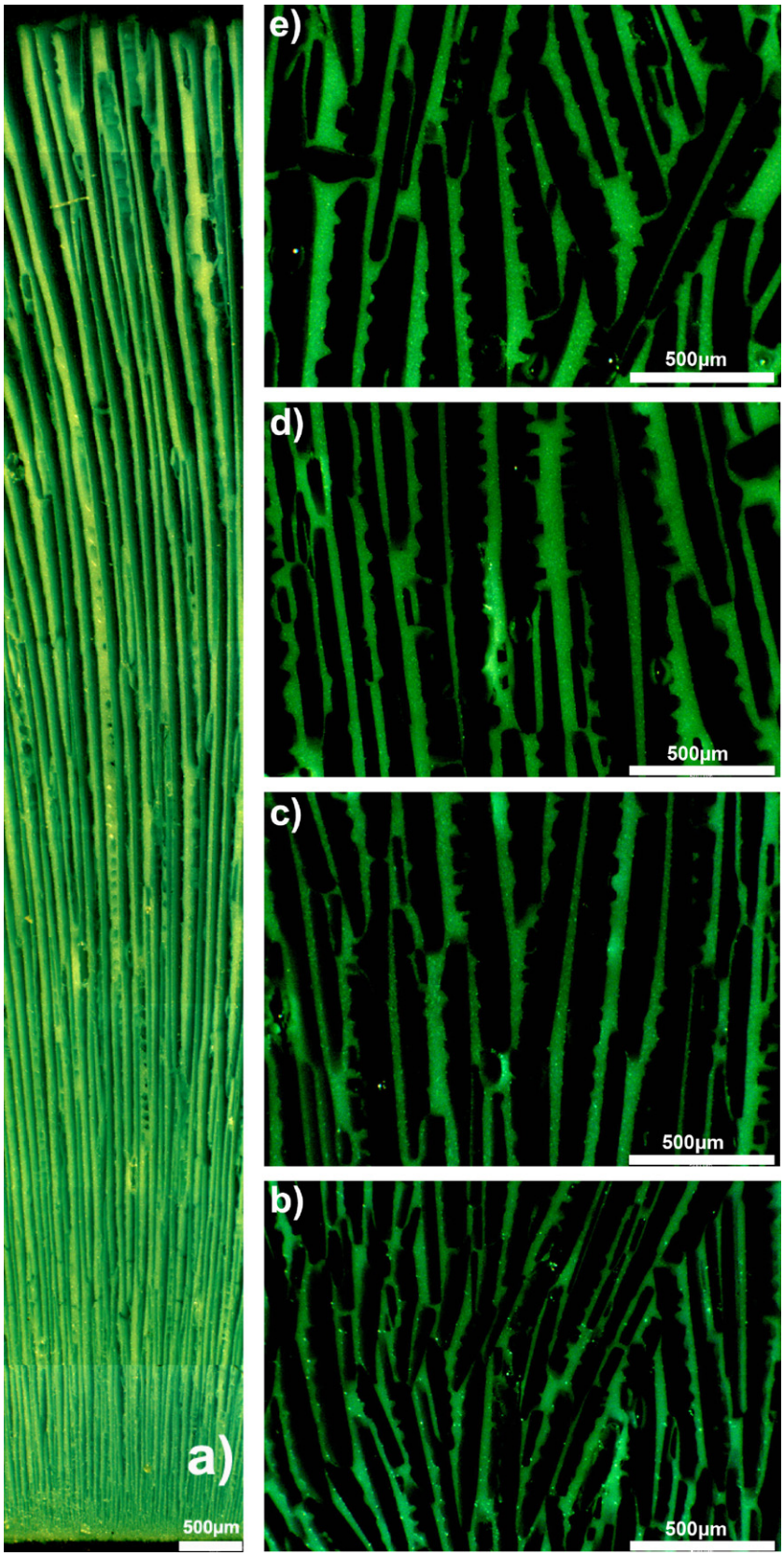

Fig. 11. Microstructure of freeze casted ceramic. (a) Cross section parallel to freezing direction, (b–e) cross section perpendicular to freezing direction at (b) 2 mm, (c) 4 mm, (d) 6 mm and (e) 8 mm distance to bottom rod. Ceramic solid content: 15 vol%, freezing conditions: top temperature: +20 °C, bottom temperature −5 °C, cooling rate: 1 °C/min.

of temperature gradient on freezing velocity was low. But when the bottom temperature was lowered (e.g. at −10 and −15 °C) the influence of the temperature gradient became more significant, which may suggest that a cooler starting temperature could lead to faster freezing as it was closer to the freezing temperature of the suspension. These findings provide some guidance for tailoring the graded pore structure in ceramics.

The evaluation of ceramic specimen with different solid contents showed, that for ceramics with high graded pore structures, lower solid content is desirable as the graded pore structure decreases in a sample with higher solid content (Fig. 7). The effect of different cooling rates (Fig. 10a) indicates that a lower rate could help to build up large gradient structures. At the same time the temperature gradient should not be significantly too high since it is also dependent on the freezing velocity, which results in smaller wavelengths.

The largest graded pore structure was achieved using a 15 vol% suspension with a temperature regime on the top rod of +20 °C and at the bottom rod of −5 °C with a cooling rate of 1 °C/min. The microstructure of cross-sections of sintered ceramics parallel and perpendicular to the freezing direction are shown in Fig. 11. As can be seen, the wavelength increases from 45 to 115 μm at 2 and 8 mm distance, respectively.

4. Discussion

Through the aid of the clear window it was possible to monitor the time for solidification. It was shown that with increasing solid content in suspension, the degree of supercooling decreased. This phenomenon is associated with the higher volume fraction of solids in suspension, leading to a higher number of nucleation sites which causes earlier nucleation. The increased solid content also raised the freezing velocity of the ice front. Three reasons explain this trend. Firstly, in suspensions with a higher solid content less water needs to be frozen, which leads to faster freezing. Secondly, with a lower water content, less crystallisation heat needs to be conveyed and thirdly, the heat conductivity of water is lower than that of ceramic particles.[30,31]

The introduction of EPD prior to freeze casting had the effect to force the ceramic particles towards the bottom of the mould in order to create an enhanced dense layer. Gas formation could be avoided through a pulsed electric field and the dense layer increased in density and thickness, but the graded pore structure decreased in the whole ceramic sample and the macrostructure became significantly finer. That is associated to the increased amount of particles on the bottom of the mould where nucleation starts.

5. Conclusion

The study showed that the microstructure of freeze casted ceramics could be tailored by controlling the solid content of the ceramic suspension and the freezing conditions. It was shown that the freezing velocity of the ice front was a crucial factor which was in turn affected by the solid content of the suspension, the pre-set temperature and the applied cooling rate. In order to achieve a significant graded pore structure in the ZTA ceramic, it has been shown that the ideal suspension had a solid content of 15 vol%. The optimal temperature settings, using the double-side controlled apparatus, were +20 °C on the top and −5 °C on the bottom rod with a cooling rate of 1 °C/min. Maximum wavelengths up to 115 μm could be achieved at a height of 11 mm. The introduction of EPD showed that the density of the dense layer could be enhanced and also the thickness, but the final microstructure was affected by it. Pulsed EPD led to a finer lamellar structure and a decrease in wavelength gradient over the whole height. Additionally, it has been shown that the degree of supercooling was considerable dependent on the solid content of suspension. With an increased solid content the temperature at which freezing started was reduced, resulting in a decrease in wavelength and in an increase in wall thickness of lamellae at the same time.

Acknowledgements

The authors wish to thanks Great Western Research (GWR) and Corin Ltd. for providing the financial support, Graham Leigh for building the apparatus and Dr. Peter Ellison for advice in the early stage of this project.

References

1. Hu L, Wang CA, Huang Y, Sun C, Lu S, Hu Z. Control of pore channel size during freeze casting of porous YSZ ceramics with unidirectionally aligned channels using different freezing temperatures. *Journal of the European Ceramic Society* 2010;**30**(16):3389–96.
2. Bettge M, Niculescu H, Gielisse PJ. Engineered porous ceramics using a directional freeze-drying process. In: *28th International Spring Seminar on Electronics Technology*. 2005. p. 12–8.
3. Barg S, Koch D, Grathwohl G. Processing and properties of graded ceramic filters. *Journal of the American Ceramic Society* 2009;**92**(12):2854–60.
4. Deville S, Saiz E, Tomsia AP. Ice-templated porous alumina structures. *Acta Materialia* 2007;**55**(6):1965–74.
5. Fukasawa T, Deng ZY, Ando M, Ohji T, Goto Y. Pore structure of porous ceramics synthesized from water-based slurry by freeze-dry process. *Journal of Materials Science* 2001;**36**(10):2523–7.
6. Koh YH, Jun IK, Sun JJ, Kim HE. In situ fabrication of a dense/porous bi-layered ceramic composite using freeze casting of a ceramic-camphene slurry. *Journal of the American Ceramic Society* 2006;**89**(2):763–6.
7. Heilmann F, Standard O, Müller F, Hoffman M. Development of graded hydroxyapatite/CaCO(3) composite structures for bone ingrowth. *Journal of Materials Science: Materials in Medicine* 2007;**18**(9):1817–24.
8. Colombo P. Conventional and novel processing methods for cellular ceramics. *Philosophical Transactions of the Royal Society A: Mathematical Physical and Engineering Sciences* 2006;**364**(1838):109–24.
9. Studart AR, Gonzenbach UT, Tervoort E, Gauckler LJ. Processing routes to macroporous ceramics: a review. *Journal of the American Ceramic Society* 2006;**89**(6):1771–89.
10. Colombo, Hellmann P, John. Ceramic foams from preceramic polymers. *Materials Research Innovations* 2002;**6**(5):260–72.
11. Deville S. Freeze-casting of porous ceramics: a review of current achievements and issues. *Advanced Engineering Materials* 2008;**10**(3):155–69.
12. Launey ME, Munch E, Alsem DH, Barth HB, Saiz E, Tomsia AP, et al. Designing highly toughened hybrid composites through nature-inspired hierarchical complexity. *Acta Materialia* 2009;**57**(10):2919–32.
13. Jung HD, Yook SW, Kim HE, Koh YH. Fabrication of titanium scaffolds with porosity and pore size gradients by sequential freeze casting. *Materials Letters* 2009;**63**(17):1545–7.
14. Li JC, Dunand DC. Mechanical properties of directionally freeze-cast titanium foams. *Acta Materialia* 2010;**59**(1):146–58.

15. Colard CAL, Cave RA, Grossiord N, Covington JA, Bon SAF. Conducting nanocomposite polymer foams from ice-crystal-templated assembly of mixtures of colloids. *Advanced Materials* 2009;**21**(28):2894–8.
16. Yoon BH, Choi WY, Kim HE, Kim JH, Koh YH. Aligned porous alumina ceramics with high compressive strengths for bone tissue engineering. *Scripta Materialia* 2008;**58**(7):537–40.
17. Deville S, Saiz E, Tomsia AP. Freeze casting of hydroxyapatite scaffolds for bone tissue engineering. *Biomaterials* 2006;**27**(32):5480–9.
18. Munch E, Launey ME, Alsem DH, Saiz E, Tomsia AP, Ritchie RO. Tough: bio-inspired hybrid materials. *Science* 2008;**322**(5907):1516–20.
19. Fukasawa T, Ando M, Ohji T, Kanzaki S. Synthesis of porous ceramics with complex pore structure by freeze-dry processing. *Journal of the American Ceramic Society* 2001;**84**(1):230–2.
20. Fukasawa T, Deng ZY, Ando M, Ohji T, Kanzaki S. Synthesis of porous silicon nitride with unidirectionally aligned channels using freeze-drying process. *Journal of the American Ceramic Society* 2002;**85**(9): 2151–5.
21. Fu Q, Rahaman MN, Dogan F, Bal BS. Freeze-cast hydroxyapatite scaffolds for bone tissue engineering applications. *Biomedical Materials* 2008;**3**(2):1–7.
22. Chino Y, Dunand David C. Directionally freeze-cast titanium foam with aligned: elongated pores. *Acta Materialia* 2008;**56**(1):105–13.
23. Li J, Zuo KH, Liu WJ, Zeng YP, Zhang FQ, Jiang DL. Porous Al_2O_3 prepared via freeze casting and its biocompatibility. In: Jiang DL, Zeng YP, Singh M, Heinrich J, editors. *Ceramic Materials and Components for Energy and Environmental Applications*. Westerville: Amer Ceramic Soc; 2010. p. 537–43.
24. Deville S, Saiz E, Nalla RK, Tomsia AP. Freezing as a path to build complex composites. *Science and Technology of Advanced Materials* 2006;**311**:515–8.
25. Waschkies T, Oberacker R, Hoffmann MJ. Control of lamellae spacing during freeze casting of ceramics using double-side cooling as a novel processing route. *Journal of the American Ceramic Society* 2009;**92**(1):S79–84.
26. Zhang YM, Hu LY, Han JC. Preparation of a dense/porous bilayered ceramic by applying an electric field during freeze casting. *Journal of the American Ceramic Society* 2009;**92**(8):1874–6.
27. Yoon HJ, Kim UC, Kim JH, Koh YH, Choi WY, Kim HE. Macroporous alumina ceramics with aligned microporous walls by unidirectionally freezing foamed aqueous ceramic suspensions. *Journal of the American Ceramic Society* 2010;**93**(6):1580–2.
28. Sofie SW. Fabrication of functionally graded and aligned porosity in thin ceramic substrates with the novel freeze-tape-casting process. *Journal of the American Ceramic Society* 2007;**90**(7):2024–31.
29. Peppin SSL, Elliott JAW, Grae Worster M. Solidification of colloidal suspensions. *Journal of Fluid Mechanics* 2006;**554**:147–66.
30. Nývlt J. *Solid–Liquid Phase Equilibria*. Elsevier Scientific; 1977.
31. Nývlt J. Nucleation and growth rate in mass crystallization. *Progress in Crystal Growth and Characterization* 1984;**9**(3–4):335–70.